Eur. Phys. J. C 52, 255–265 (2007)
DOI 10.1140/epjc/s10052-007-0376-6

THE EUROPEAN PHYSICAL JOURNAL C

Regular Article – Experimental Physics

Double spin asymmetry in exclusive ρ^0 muoproduction at COMPASS

The COMPASS Collaboration

M. Alekseev[29], V.Yu. Alexakhin[8], Yu. Alexandrov[18], G.D. Alexeev[8], A. Amoroso[29], A. Arbuzov[8], B. Badełek[30], F. Balestra[29], J. Ball[25], G. Baum[1], J. Barth[4], Y. Bedfer[25], C. Bernet[25], R. Bertini[29], M. Bettinelli[19], R. Birsa[28], J. Bisplinghoff[3], P. Bordalo[15,a], F. Bradamante[28], A. Bravar[16], A. Bressan[28], G. Brona[30], E. Burtin[25], M.P. Bussa[29], A. Chapiro[27], M. Chiosso[29], A. Cicuttin[27], M. Colantoni[29,b], S. Costa[29], M.L. Crespo[27], N. d'Hose[25], S. Dalla Torre[28], S. Das[7], S.S. Dasgupta[6], R. De Masi[20], N. Dedek[19], O.Yu. Denisov[29,c], L. Dhara[7], V. Diaz[27], A.M. Dinkelbach[20], S.V. Donskov[24], V.A. Dorofeev[24], N. Doshita[21], V. Duic[28], W. Dünnweber[19], P.D. Eversheim[3], W. Eyrich[9], M. Fabro[28], M. Faessler[19], V. Falaleev[11], A. Ferrero[29], L. Ferrero[29], M. Finger[22], M. Finger jr.[8], H. Fischer[10], C. Franco[15], J. Franz[10], J.M. Friedrich[20], V. Frolov[29,c], R. Garfagnini[29], F. Gautheron[1], O.P. Gavrichtchouk[8], R. Gazda[30], S. Gerassimov[18,20], R. Geyer[19], M. Giorgi[28], B. Gobbo[28], S. Goertz[2,4], A.M. Gorin[24], S. Grabmüller[20], O.A. Grajek[30], A. Grasso[29], B. Grube[20], R. Gushterski[8], A. Guskov[8], F. Haas[20], J. Hannappel[4], D. von Harrach[16], T. Hasegawa[17], J. Heckmann[2], S. Hedicke[10], F.H. Heinsius[10], R. Hermann[16], C. Heß[2], F. Hinterberger[3], M. von Hodenberg[10], N. Horikawa[21,d], S. Horikawa[21], C. Ilgner[19], A.I. Ioukaev[8], S. Ishimoto[21], O. Ivanov[8], Yu. Ivanshin[8], T. Iwata[21,32], R. Jahn[3], A. Janata[8], P. Jasinski[16], R. Joosten[3], N.I. Jouravlev[8], E. Kabuß[16], D. Kang[10], B. Ketzer[20], G.V. Khaustov[24], Yu.A. Khokhlov[24], Yu. Kisselev[1,2], F. Klein[4], K. Klimaszewski[30], S. Koblitz[16], J.H. Koivuniemi[13], V.N. Kolosov[24], E.V. Komissarov[8], K. Kondo[21], K. Königsmann[10], I. Konorov[18,20], V.F. Konstantinov[24], A.S. Korentchenko[8], A. Korzenev[16,c], A.M. Kotzinian[8,29], N.A. Koutchinski[8], O. Kouznetsov[8,25], N.P. Kravchuk[8], A. Kral[23], Z.V. Kroumchtein[8], R. Kuhn[20], F. Kunne[25], K. Kurek[30], M.E. Ladygin[24], M. Lamanna[11,28], J.M. Le Goff[25], A.A. Lednev[24], A. Lehmann[9], J. Lichtenstadt[26], T. Liska[23], I. Ludwig[10], A. Maggiora[29], M. Maggiora[29], A. Magnon[25], G.K. Mallot[11,e], A. Mann[20], C. Marchand[25], J. Marroncle[25], A. Martin[28], J. Marzec[31], F. Massmann[3], T. Matsuda[17], A.N. Maximov[8], W. Meyer[2], A. Mielech[28,30], Yu.V. Mikhailov[24], M.A. Moinester[26], A. Mutter[10,16], O. Nähle[3], A. Nagaytsev[8], T. Nagel[20], J. Nassalski[30], S. Neliba[23], F. Nerling[10], S. Neubert[20], D.P. Neyret[25], V.I. Nikolaenko[24], K. Nikolaev[8], A.G. Olshevsky[8], M. Ostrick[4], A. Padee[31], P. Pagano[28], S. Panebianco[25], R. Panknin[4], D. Panzieri[29,b], S. Paul[20], B. Pawlukiewicz-Kaminska[30], D.V. Peshekhonov[8], V.D. Peshekhonov[8], G. Piragino[29], S. Platchkov[25], J. Pochodzalla[16], J. Polak[14], V.A. Polyakov[24], J. Pretz[4], S. Procureur[25], C. Quintans[15], J.-F. Rajotte[19], V. Rapatsky[8], S. Ramos[15,a], G. Reicherz[2], A. Richter[9], F. Robinet[25], E. Rocco[28,29], E. Rondio[30], A.M. Rozhdestvensky[8], D.I. Ryabchikov[24], V.D. Samoylenko[24], A. Sandacz[30], H. Santos[15], M.G. Sapozhnikov[8], S. Sarkar[7], I.A. Savin[8], P. Schiavon[28], C. Schill[10], L. Schmitt[20], P. Schönmeier[9], W. Schröder[9], O.Yu. Shevchenko[8], H.-W. Siebert[12,16], L. Silva[15], L. Sinha[7], A.N. Sissakian[8], M. Slunecka[8], G.I. Smirnov[8], S. Sosio[29], F. Sozzi[28], V.P. Sugonyaev[24], A. Srnka[5], F. Stinzing[9], M. Stolarski[30,10], M. Sulc[14], R. Sulej[31], N. Takabayashi[21], V.V. Tchalishev[8], S. Tessaro[28], F. Tessarotto[28], A. Teufel[9], L.G. Tkatchev[8], G. Venugopal[3], M. Virius[23], N.V. Vlassov[8], A. Vossen[10], R. Webb[9], E. Weise[3], Q. Weitzel[20], R. Windmolders[4], S. Wirth[9], W. Wiślicki[30], K. Zaremba[31], M. Zavertyaev[18], E. Zemlyanichkina[8], J. Zhao[16], R. Ziegler[3], A. Zvyagin[19]

[1] Universität Bielefeld, Fakultät für Physik, 33501 Bielefeld, Germany[f]
[2] Universität Bochum, Institut für Experimentalphysik, 44780 Bochum, Germany[f]
[3] Universität Bonn, Helmholtz-Institut für Strahlen- und Kernphysik, 53115 Bonn, Germany[f]
[4] Universität Bonn, Physikalisches Institut, 53115 Bonn, Germany[f]
[5] Institute of Scientific Instruments, AS CR, 61264 Brno, Czech Republic[g]
[6] Burdwan University, Burdwan 713104, India[h]
[7] Matrivani Institute of Experimental Research & Education, Calcutta-700 030, India[i]
[8] Joint Institute for Nuclear Research, 141980 Dubna, Moscow region, Russia
[9] Universität Erlangen–Nürnberg, Physikalisches Institut, 91054 Erlangen, Germany[f]
[10] Universität Freiburg, Physikalisches Institut, 79104 Freiburg, Germany[f]
[11] CERN, 1211 Geneva 23, Switzerland
[12] Universität Heidelberg, Physikalisches Institut, 69120 Heidelberg, Germany[f]
[13] Helsinki University of Technology, Low Temperature Laboratory, 02015 HUT, Finland and University of Helsinki, Helsinki Institute of Physics, 00014 Helsinki, Finland
[14] Technical University in Liberec, 46117 Liberec, Czech Republic[g]

[15] LIP, 1000-149 Lisbon, Portugal[j]
[16] Universität Mainz, Institut für Kernphysik, 55099 Mainz, Germany[f]
[17] University of Miyazaki, Miyazaki 889-2192, Japan[k]
[18] Lebedev Physical Institute, 119991 Moscow, Russia
[19] Ludwig-Maximilians-Universität München, Department für Physik, 80799 Munich, Germany[f]
[20] Technische Universität München, Physik Department, 85748 Garching, Germany[f]
[21] Nagoya University, 464 Nagoya, Japan[j]
[22] Charles University, Faculty of Mathematics and Physics, 18000 Prague, Czech Republic[g]
[23] Czech Technical University in Prague, 16636 Prague, Czech Republic[g]
[24] State Research Center of the Russian Federation, Institute for High Energy Physics, 142281 Protvino, Russia
[25] CEA DAPNIA/SPhN Saclay, 91191 Gif-sur-Yvette, France
[26] Tel Aviv University, School of Physics and Astronomy, 69978 Tel Aviv, Israel[l]
[27] ICTP–INFN MLab Laboratory, 34014 Trieste, Italy
[28] INFN Trieste and University of Trieste, Department of Physics, 34127 Trieste, Italy
[29] INFN Turin and University of Turin, Physics Department, 10125 Turin, Italy
[30] Sołtan Institute for Nuclear Studies and Warsaw University, 00-681 Warsaw, Poland[m]
[31] Warsaw University of Technology, Institute of Radioelectronics, 00-665 Warsaw, Poland[n]
[32] Yamagata University, Yamagata, 992-8510 Japan[k]

Received: 14 April 2007 / Revised version: 10 July 2007 /
Published online: 16 August 2007 –

Abstract. The longitudinal double spin asymmetry A_1^ρ for exclusive leptoproduction of ρ^0 mesons, $\mu + N \to \mu + N + \rho$, is studied using the COMPASS 2002 and 2003 data. The measured reaction is incoherent exclusive ρ^0 production on polarised deuterons. The Q^2 and x dependence of A_1^ρ is presented in a wide kinematical range, $3 \times 10^{-3} < Q^2 < 7\,(\mathrm{GeV}/c)^2$ and $5 \times 10^{-5} < x < 0.05$. The results presented are the first measurements of A_1^ρ at small Q^2 ($Q^2 < 0.1\,(\mathrm{GeV}/c)^2$) and small x ($x < 3 \times 10^{-3}$). The asymmetry is in general compatible with zero in the whole kinematical range.

PACS. 13.60.Le; 13.88.+e

1 Introduction

In this paper we present results on the longitudinal double spin asymmetry A_1^ρ for exclusive incoherent ρ^0 production in the scattering of high energy muons on nucleons. The experiment was carried out at CERN by the COMPASS collaboration using the 160 GeV muon beam and the large ^{6}LiD polarised target.

The reaction studied is

$$\mu + N \to \mu' + \rho^0 + N' \,, \tag{1}$$

where N is a quasi-free nucleon from the polarised deuterons. The reaction (1) can be described in terms of the virtual photoproduction process

$$\gamma^* + N \to \rho^0 + N' \,. \tag{2}$$

The reaction (2) can be regarded as a fluctuation of the virtual photon into a quark–antiquark pair (in partonic language), or an off-shell vector meson (in the vector meson dominance model), which then scatters off the target nucleon, resulting in the production of an on-shell vector meson. At high energies this is predominantly a diffractive process and plays an important role in the investigation of Pomeron exchange and its interpretation in terms of multiple gluon exchange.

[a] Also at IST, Universidade Técnica de Lisboa, Lisbon, Portugal
[b] Also at University of East Piedmont, 15100 Alessandria, Italy
[c] On leave of absence from JINR Dubna
[d] Also at Chubu University, Kasugai, Aichi, 487-8501 Japan
[e] e-mail: gerhard.mallot@cern.ch
[f] Supported by the German Bundesministerium für Bildung und Forschung
[g] Suppported by Czech Republic MEYS grants ME492 and LA242
[h] Supported by DST-FIST II grants, Govt. of India
[i] Supported by the Shailabala Biswas Education Trust
[j] Supported by the Portuguese FCT - Fundação para a Ciência e Tecnologia grants POCTI/FNU/49501/2002 and POCTI/FNU/50192/2003
[k] Supported by the Ministry of Education, Culture, Sports, Science and Technology, Japan; Daikou Foundation and Yamada Foundation
[l] Supported by the Israel Science Foundation, founded by the Israel Academy of Sciences and Humanities
[m] Supported by KBN grant nr 621/E-78/SPUB-M/CERN/P-03/DZ 298 2000, nr 621/E-78/SPB/CERN/P-03/DWM 576/2003-2006, and by MNII reasearch funds for 2005–2007
[n] Supported by KBN grant nr 134/E-365/SPUB-M/CERN/P- 03/DZ299/2000

Most of the presently available information on the spin structure of reaction (2) stems from the ρ^0 spin density matrix elements, which are obtained from the analysis of the angular distributions of ρ^0 production and decay [1]. Experimental results on ρ^0 spin density matrix elements come from various experiments [2–7], including the preliminary results from COMPASS [8].

The emerging picture of the spin structure of the process considered is the following. At low photon virtuality Q^2 the cross section by transverse virtual photons σ_{T} dominates, while the relative contribution of the cross section by longitudinal photons σ_{L} rapidly increases with Q^2. At a Q^2 of about $2\,(\mathrm{GeV}/c)^2$ both components become comparable and at a larger Q^2 the contribution of σ_{L} becomes dominant and continues to grow, although at a lower rate than at a low Q^2. Approximately, the so called s-channel helicity conservation (SCHC) is valid, i.e. the helicity of the vector meson is the same as the helicity of the parent virtual photon. The data indicate that the process can be described approximately by the exchange in the t-channel of an object with natural parity P. Small deviations from SCHC are observed, also at the highest energies, whose origin is still to be understood. The interesting suggestion was made in [9, 10] that at high energies the magnitudes of various helicity amplitudes for the reaction (2) may shed light on the spin–orbital momentum structure of the vector meson.

Complementary information can be obtained from measurements of the double spin cross section asymmetry, when information on both the beam and target polarisation is used. The asymmetry is defined as

$$A_1^\rho = \frac{\sigma_{1/2} - \sigma_{3/2}}{\sigma_{1/2} + \sigma_{3/2}}, \tag{3}$$

where $\sigma_{1/2\,(3/2)}$ stands for the cross sections of the reaction (2), and the subscripts denote the total virtual photon–nucleon angular momentum component along the virtual-photon direction. In the following we will also use the asymmetry A_{LL}, which is defined for reaction (1) as the asymmetry of the muon–nucleon cross sections for antiparallel and parallel beam and target longitudinal spin orientations.

In the Regge approach [11] the longitudinal double spin asymmetry A_1^ρ can arise due to the interference of the amplitudes for exchange in the t-channel of Reggeons with natural parity (Pomeron, ρ, ω, f, A_2) with the amplitudes for Reggeons with unnatural parity (π, A_1). No significant asymmetry is expected when only a non-perturbative Pomeron is exchanged, because it has small spin dependent couplings as found from hadron–nucleon data for cross sections and polarisations.

Similarly, in the approach of Fraas [12], assuming the approximate validity of SCHC, the spin asymmetry A_1^ρ arises from the interference between parts of the helicity amplitudes for transverse photons corresponding to the natural- and unnatural-parity exchanges in the t-channel. While a measurable asymmetry can arise even from a small contribution of the unnatural-parity exchange, the latter may remain unmeasurable in the cross sections. A significant unnatural-parity contribution may indicate exchange of certain Reggeons like π and A_1 or in partonic terms an exchange of $q\bar{q}$ pairs.

In the same reference a theoretical prediction for A_1^ρ was presented, which is based on the description of forward exclusive ρ^0 leptoproduction and inclusive inelastic lepton–nucleon scattering by the off-diagonal generalised vector meson dominance (GVMD) model, applied to the case of polarised lepton–nucleon scattering. At the values of the Bjorken variable $x < 0.2$, with additional assumptions [13], A_1^ρ can be related to the A_1 asymmetry for inclusive inelastic lepton scattering at the same x as

$$A_1^\rho = \frac{2A_1}{1 + (A_1)^2}. \tag{4}$$

This prediction is consistent with the HERMES results for both proton and deuteron targets, although with rather large errors.

In perturbative QCD, there exists a general proof of factorisation [14] for exclusive vector meson production by longitudinal photons. It allows for a decomposition of the full amplitude for reaction (2) into three components: a hard scattering amplitude for the exchange of quarks or gluons, a distribution amplitude for the meson and the non-perturbative description of the target nucleon in terms of the generalised parton distributions (GPDs), which are related to the internal structure of the nucleon. No similar proof of factorisation exists for transverse virtual photons, and as a consequence the interpretation of A_1^ρ in perturbative QCD is not possible at leading twist. However, a model including higher twist effects proposed by Martin et al. [15] describes the behaviour of both σ_{L} as well as of σ_{T} reasonably well. An extension of this model by Ryskin [16] for the spin dependent cross sections allows one to relate A_1^ρ to the spin dependent GPDs of gluons and quarks in the nucleon. The applicability of this model is limited to the range $Q^2 \geq 4\,(\mathrm{GeV}/c)^2$. More recently another pQCD-inspired model involving GPDs has been proposed by Goloskokov and Kroll [17, 18]. The non-leading twist asymmetry A_{LL} results from the interference between the dominant GPD H_g and the helicity dependent GPD $\tilde{H}_g$. The asymmetry is estimated to be of the order $k_{\mathrm{T}}^2 \tilde{H}_g / \left(Q^2 H_g\right)$, where k_{T} is the transverse momentum of the quark and the antiquark.

Up to now little experimental information has been available on the double spin asymmetries for exclusive leptoproduction of vector mesons. The first observation of a non-zero asymmetry A_1^ρ in polarised electron–proton deep-inelastic scattering was reported by the HERMES experiment [13]. In the deep inelastic region ($0.8 < Q^2 < 3\,(\mathrm{GeV}/c)^2$) the measured asymmetry is equal to $0.23 \pm 0.14\,(\mathrm{stat}) \pm 0.02\,(\mathrm{syst})$ [19], with little dependence on the kinematical variables. In contrast, for the 'quasi-real photoproduction' data, with $\langle Q^2 \rangle = 0.13\,(\mathrm{GeV}/c)^2$, the asymmetry for the proton target is consistent with zero. On the other hand the measured asymmetry A_1^ρ for the polarised deuteron target and the asymmetry A_1^ϕ for exclusive production of ϕ meson either on polarised protons or deuterons are consistent with zero both in the deep inelastic and in the quasi-real photoproduction regions [19].

The HERMES result indicating a non-zero A_1^ρ for the proton target differs from the unpublished result of similar measurements by the SMC experiment [20] at comparable values of Q^2 but at about three times higher values of the photon–nucleon centre of mass energy W, i.e. at smaller x. The SMC measurements of $A_{\rm LL}$ in several bins of Q^2 are consistent with zero for both proton and deuteron targets.

2 The experimental set-up

The experiment [21] was performed with the high intensity positive muon beam from the CERN M2 beam line. The μ^+ beam intensity is 2×10^8 per spill of 4.8 s with a cycle time of 16.8 s. The average beam energy is 160 GeV and the momentum spread is $\sigma_p/p = 0.05$. The momentum of each beam muon is measured upstream of the experimental area in a beam momentum station consisting of several planes of scintillator strips or scintillating fibres with a dipole magnet in between. The precision of the momentum determination is typically $\Delta p/p \leq 0.003$. The μ^+ beam is naturally polarised by the weak decays of the parent hadrons. The polarisation of the muon varies with its energy and the average polarisation is -0.76.

The beam traverses the two cells of the polarised target, each 60 cm long, 3 cm in diameter and separated by 10 cm, which are placed one after the other. The target cells are filled with ^{6}LiD, which is used as polarised deuteron target material and is longitudinally polarised by dynamic nuclear polarisation (DNP). The two cells are polarised in opposite directions so that data from both spin directions are recorded at the same time. The typical values of polarisation are about 0.50. A mixture of liquid ^{3}He and ^{4}He, used to refrigerate the target, and a small amount of heavier nuclei are also present in the target. The spin directions in the two target cells are reversed every 8 h by rotating the direction of the magnetic field in the target. In this way fluxes and acceptances cancel in the calculation of spin asymmetries, provided that the ratio of acceptances of the two cells remains unchanged after the reversal.

The COMPASS spectrometer is designed to reconstruct the scattered muons and the produced hadrons in wide momentum and angular ranges. It is divided in two stages with two dipole magnets, SM1 and SM2. The first magnet, SM1, accepts charged particles of momenta larger than $0.4\,{\rm GeV}/c$, and the second one, SM2, those larger than $4\,{\rm GeV}/c$. The angular acceptance of the spectrometer is limited by the aperture of the polarised target magnet. For the upstream end of the target it is ± 70 mrad.

To match the expected particle flux at various locations in the spectrometer, COMPASS uses various tracking detectors. Small-angle tracking is provided by stations of scintillating fibres, silicon detectors, micromesh gaseous chambers and gas electron multiplier chambers. Large-angle tracking devices are multiwire proportional chambers, drift chambers and straw detectors. Muons are identified in large-area mini drift tubes and drift tubes placed downstream of hadron absorbers. Hadrons are detected by two large iron-scintillator sampling calorimeters, installed in front of the absorbers and shielded to avoid electromagnetic contamination. The identification of charged particles is possible with a RICH detector, although in this paper we have not utilised the information from the RICH.

The data recording system is activated by various triggers indicating the presence of a scattered muon and/or energy deposited by hadrons in the calorimeters. In addition to the inclusive trigger, in which the scattered muon is identified by coincidence signals in the trigger hodoscopes, several semi-inclusive triggers were used. They select events fulfilling the requirement to detect the scattered muon together with the energy deposited in the hadron calorimeters exceeding a given threshold. In 2003 the acceptance was further extended towards high Q^2 values by the addition of a stand-alone calorimetric trigger in which no condition is set for the scattered muon. The COMPASS trigger system allows us to cover a wide range of Q^2, from quasi-real photoproduction to deep inelastic interactions.

A more detailed description of the COMPASS apparatus can be found in [21].

3 Event sample

For the present analysis the whole data sample taken in 2002 and 2003 with the longitudinally polarised target is used. For an event to be accepted for further analysis it is required to originate in the target, have a reconstructed beam track, a scattered muon track, and only two additional tracks of oppositely charged hadrons associated to the primary vertex. The fluxes of beam muons passing through each target cell are equalised using appropriate cuts on the position and angle of the beam tracks.

The charged pion mass hypothesis is assigned to each hadron track and the invariant mass of two pions, $m_{\pi\pi}$, calculated. A cut on the invariant mass of two pions, $0.5 < m_{\pi\pi} < 1\,{\rm GeV}/c^2$, is applied to select the ρ^0. As slow recoil target particles are not detected, in order to select exclusive events we use the cut on the missing energy, $-2.5 < E_{\rm miss} < 2.5$ GeV, and on the transverse momentum of ρ^0 with respect to the direction of virtual photon, $p_{\rm t}^2 < 0.5\,({\rm GeV}/c)^2$. Here $E_{\rm miss} = \left(M_X^2 - M_p^2\right)/2M_p$, where M_X is the missing mass of the unobserved recoiling system and M_p is the proton mass. Coherent interactions on the target nuclei are removed by a cut $p_{\rm t}^2 > 0.15\,({\rm GeV}/c)^2$. To avoid large corrections for acceptance and misidentification of events, the additional cuts $\nu > 30$ GeV and $E_{\mu'} > 20$ GeV are applied.

The distributions of $m_{\pi\pi}$, $E_{\rm miss}$ and $p_{\rm t}^2$ are shown in Fig. 1. Each plot is obtained applying all cuts except those corresponding to the displayed variable. On the left top panel of Fig. 1 a clear peak of the ρ^0 resonance, centred at $770\,{\rm MeV}/c^2$, is visible on top of the small contribution of background of the non-resonant $\pi^+\pi^-$ pairs. Also the skewing of the resonance peak towards smaller values of $m_{\pi\pi}$, due to interference with the non-resonant background, is noticeable. A small bump below $0.4\,{\rm GeV}/c^2$ is due to assignment of the charged pion mass to the kaons from decays of ϕ mesons. The mass cuts eliminate the non-

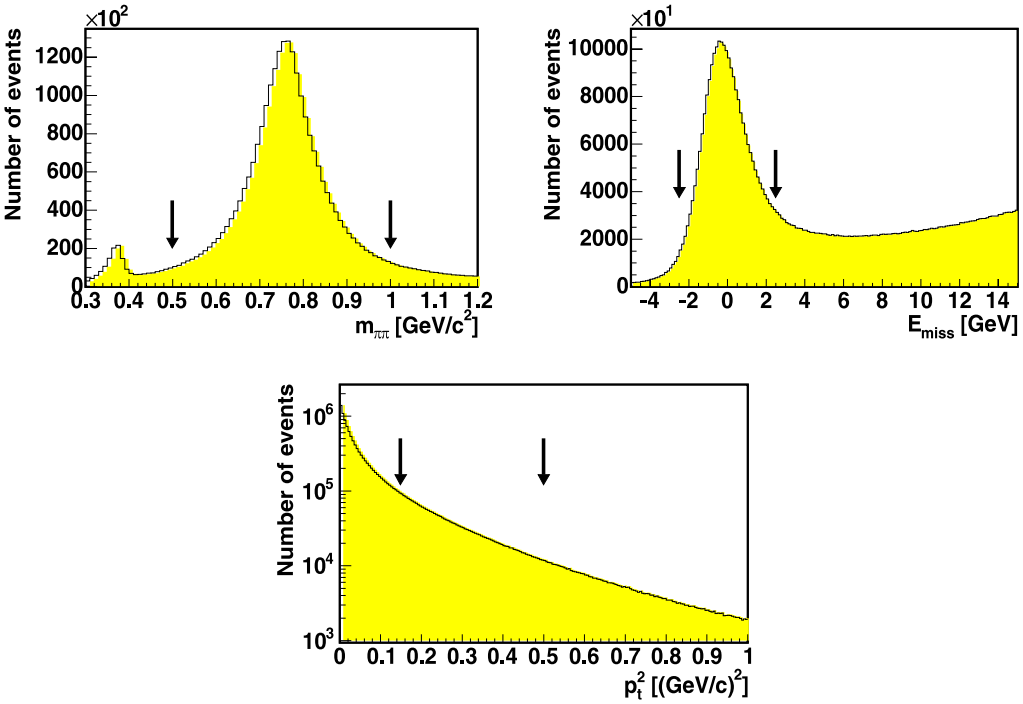

Fig. 1. Distributions of $m_{\pi\pi}$ (*upper left*), $E_{\rm miss}$ (*upper right*) and p_t^2 (*lower*) for the exclusive sample. The *arrows* show cuts imposed on each variable to define the final sample

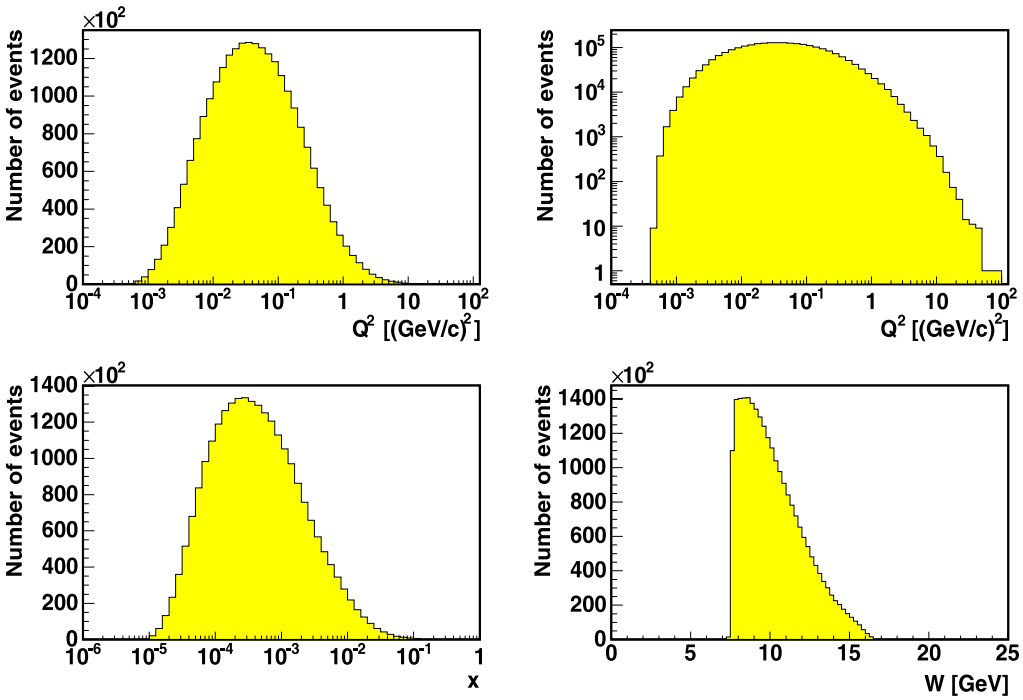

Fig. 2. Distributions of the kinematical variables for the final sample (in reading order): Q^2 with linear and logarithmic vertical axis scale, x, and the energy W

resonant background outside of the ρ^0 peak as well as the contribution of ϕ mesons.

On the right top panel of the figure the peak at $E_{\rm miss} \approx 0$ is the signal of exclusive ρ^0 production. The width of the peak, $\sigma \approx 1.1$ GeV, is due to the resolution of the spectrometer. Non-exclusive events, where in addition to the recoil nucleon other undetected hadrons are produced, appear at $E_{\rm miss} > 0$. Due to the finite resolution, however, they are not resolved from the exclusive peak. This background consists of two components: the double-diffractive events where additionally to ρ^0 an excited nucleon state is produced in the nucleon vertex of reaction (2), and events with semi-inclusive ρ^0 production, in which other hadrons are produced but escape detection.

The $p_{\rm t}^2$ distribution shown on the bottom panel of the figure indicates a contribution from coherent production on target nuclei at small $p_{\rm t}^2$ values. A three-exponential fit to this distribution was performed, which indicates also

a contribution of non-exclusive background increasing with p_t^2. Therefore, to select the sample of exclusive incoherent ρ^0 production, the aforementioned p_t^2 cuts, indicated by arrows, were applied.

After all selections the final sample consists of about 2.44 million events. The distributions of Q^2, x and W are shown in Fig. 2. The data cover a wide range in Q^2 and x which extends towards the small values by almost two orders of magnitude compared to the similar studies reported in [19]. The sharp edge of the W distribution at the low W values is a consequence of the cut applied on ν. For this sample $\langle W \rangle$ is equal to 10.2 GeV and $\langle p_t^2 \rangle = 0.27\,(\mathrm{GeV}/c)^2$.

4 Extraction of asymmetry A_1^ρ

The cross section asymmetry $A_{\mathrm{LL}} = (\sigma_{\uparrow\downarrow} - \sigma_{\uparrow\uparrow})/(\sigma_{\uparrow\downarrow} + \sigma_{\uparrow\uparrow})$ for reaction (1), for antiparallel ($\uparrow\downarrow$) and parallel ($\uparrow\uparrow$) spins of the incoming muon and the target nucleon, is related to the virtual-photon nucleon asymmetry A_1^ρ by

$$A_{\mathrm{LL}} = D\,(A_1^\rho + \eta A_2^\rho)\,, \tag{5}$$

where the factors D and η depend on the event kinematics, and A_2^ρ is related to the interference cross section for exclusive production by longitudinal and transverse virtual photons. As the presented results extend into the range of very small Q^2, the exact formulae for the depolarisation factor D and kinematical factor η [22] are used without neglecting terms proportional to the lepton mass squared m^2. The depolarisation factor is given by

$$D(y,Q^2) = \frac{y\left[(1+\gamma^2 y/2)(2-y) - 2y^2m^2/Q^2\right]}{y^2(1-2m^2/Q^2)(1+\gamma^2) + 2(1+R)(1-y-\gamma^2y^2/4)}, \tag{6}$$

where $R = \sigma_{\mathrm{L}}/\sigma_{\mathrm{T}}$, $\sigma_{\mathrm{L(T)}}$ is the cross section for the reaction (2) initiated by longitudinally (transversely) polarised virtual photons, the fraction of the muon energy lost $y = \nu/E_\mu$, and $\gamma^2 = Q^2/\nu^2$. The kinematical factor $\eta(y,Q^2)$ is the same as for the inclusive asymmetry.

The asymmetry A_2^ρ obeys the positivity limit $A_2^\rho < \sqrt{R}$, analogous to the one for the inclusive case. For $Q^2 \leq 0.1\,(\mathrm{GeV}/c)^2$ the ratio R for the reaction (2) is small, cf. Fig. 3, and the positivity limit constrains A_2^ρ to small values. Although for larger Q^2 the ratio R for the process (2) increases with Q^2, because of the small values of η the product $\eta\sqrt{R}$ is small in the whole Q^2 range of our sample. Therefore, the second term in (5) can be neglected, so that

$$A_1^\rho \simeq \frac{1}{D} A_{\mathrm{LL}}\,, \tag{7}$$

and the effect of this approximation is included in the systematic uncertainty of A_1^ρ.

The number of events N_i collected from a given target cell in a given time interval is related to the spin independent cross section $\bar{\sigma}$ for reaction (2) and to the asymmetry

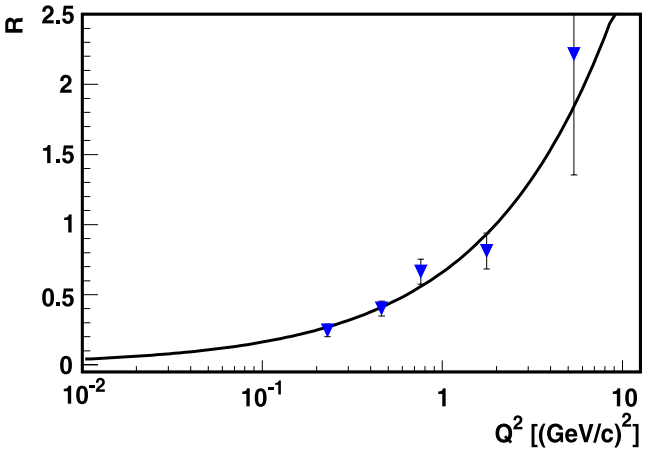

Fig. 3. The ratio $R = \sigma_{\mathrm{L}}/\sigma_{\mathrm{T}}$ as a function of Q^2 measured in the E665 experiment. The curve is a fit to the data described in the text

A_1^ρ by

$$N_i = a_i \phi_i n_i \bar{\sigma}(1 + P_{\mathrm{B}} P_{\mathrm{T}} f D A_1^\rho), \tag{8}$$

where P_{B} and P_{T} are the beam and target polarisations, ϕ_i is the incoming muon flux, a_i the acceptance for the target cell, n_i the corresponding number of target nucleons, and f the target dilution factor. The asymmetry is extracted from the data sets taken before and after reversal of the target spin directions. The four relations of (8), corresponding to the two cells (u and d) and the two spin orientations (1 and 2) lead to a second-order equation in A_1^ρ for the ratio $(N_{u,1}N_{d,2}/N_{d,1}N_{u,2})$. Here fluxes cancel out as well as acceptances, if the ratio of acceptances for the two cells is the same before and after the reversal [23]. In order to minimise the statistical error all quantities used in the asymmetry calculation are evaluated event by event with the weight factor $w = P_{\mathrm{B}} f D$. The polarisation of the beam muon, P_{B}, is obtained from a simulation of the beam line and parameterised as a function of the beam momentum. The target polarisation is not included in the event weight w because it may vary in time and generate false asymmetries. An average P_{T} is used for each target cell and each spin orientation.

The ratio R, which enters the formula for D and strongly depends on Q^2 for reaction (2), was calculated on an event-by-event basis using the parameterisation

$$R(Q^2) = a_0 (Q^2)^{a_1}, \tag{9}$$

with $a_0 = 0.66 \pm 0.05$, and $a_1 = 0.61 \pm 0.09$. The parameterisation was obtained by the Fermilab E665 experiment from a fit to their R measurements for exclusive ρ^0 muoproduction on protons [3]. These are shown in Fig. 3 together with the fitted Q^2 dependence. The preliminary COMPASS results on R for the incoherent exclusive ρ^0 production on the nucleon [8], which cover a broader kinematic region in Q^2, agree reasonably well with this parameterisation. The uncertainty of a_0 and a_1 is included in the systematic error of A_1^ρ.

The dilution factor f gives the fraction of events of reaction (2) originating from nucleons in polarised deuterons inside the target material. It is calculated event by event using the formula

$$f = C_1 f_0 = C_1 \frac{n_{\rm D}}{n_{\rm D} + \Sigma_A n_A (\tilde{\sigma}_A/\tilde{\sigma}_{\rm D})}. \qquad (10)$$

Here $n_{\rm D}$ and n_A denote numbers of nucleons in deuteron and nucleus of atomic mass A in the target, and $\tilde{\sigma}_{\rm D}$ and $\tilde{\sigma}_A$ are the cross sections per nucleon for reaction (2) occurring on the deuteron and on the nucleus of atomic mass A, respectively. The sum runs over all nuclei present in the COMPASS target. The factor C_1 takes into account that there are two polarised deuterons in the ^{6}LiD molecule, as the ^{6}Li nucleus is in first approximation composed of a deuteron and an α particle.

The measurements of the $\tilde{\sigma}_A/\tilde{\sigma}_{\rm D}$ for incoherent exclusive ρ^0 production come from the NMC [2], E665 [24] and early experiments on ρ^0 photoproduction [25]. They were fitted in [26] with the formula

$$\tilde{\sigma}_A = \sigma_p A^{\alpha(Q^2)-1}, \quad \text{with} \quad \alpha(Q^2) - 1 = -\frac{1}{3} \exp\left\{-\frac{Q^2}{Q_0^2}\right\}, \qquad (11)$$

where σ_p is the cross section for reaction (2) on the free proton. The value of the fitted parameter, Q_0^2, is equal to $9 \pm 3\,(\mathrm{GeV}/c)^2$. The measured values of the parameter α and the fitted curve $\alpha(Q^2)$ are shown on the left panel of Fig. 4 taken from [26]. On the right panel of the figure the average value of f is plotted for the various Q^2 bins used in the present analysis. The values of f are equal to about 0.36 in most of the Q^2 range, rising to about 0.38 at the highest Q^2.

The radiative corrections (RC) have been neglected in the present analysis, in particular in the calculation of f, because they are expected to be small for reaction (1). They were evaluated [27] to be of the order of 6% for the NMC exclusive ρ^0 production analysis. The small values of RC are mainly due to the requirement of event exclusivity via cuts on $E_{\rm miss}$ and $p_{\rm t}^2$, which largely suppress the dominant external photon radiation. The internal (infrared and virtual) RC were estimated in [27] to be of the order of 2%.

5 Systematic errors

The main systematic uncertainty of A_1^ρ comes from an estimate of possible false asymmetries. In order to improve the accuracy of this estimate, in addition to the standard sample of incoherent events, a second sample was selected by changing the $p_{\rm t}^2$ cuts to

$$0 < p_{\rm t}^2 < 0.5\,(\mathrm{GeV}/c)^2, \qquad (12)$$

and keeping all the remaining selections and cuts the same as for the 'incoherent sample'. In the following it will be referred to as the 'extended $p_{\rm t}^2$ sample'. Such an extension of the p_t^2 range allows one to obtain a sample that is about five times larger than the incoherent sample. However, in addition to incoherent events such a sample contains a large fraction of events originating from coherent ρ^0 production. Therefore, for the estimate of the dilution factor f a different nuclear dependence of the exclusive cross section was used, applicable for the sum of coherent and incoherent cross sections [2]. The physics asymmetries A_1^ρ for both samples are consistent within statistical errors.

Possible false experimental asymmetries were searched for by modifying the selection of data sets used for the asymmetry calculation. The grouping of the data into configurations with opposite target polarisation was varied from large samples, covering at most two weeks of data taking, into about 100 small samples, taken in time intervals of the order of 16 hours. A statistical test was performed on the distributions of asymmetries obtained from these small samples. In each of the Q^2 and x bins the dispersion of the values of A_1^ρ around their mean agrees with the statistical error. Time dependent effects that would lead to a broadening of these distributions were thus not observed. Allowing the dispersion of A_1^ρ to vary within its two standard deviations we obtain for each bin an upper bound for the systematic error arising from time dependent effects

$$\sigma_{\mathrm{false}A,t\mathrm{dep}} < 0.56\sigma_{\rm stat}. \qquad (13)$$

Here $\sigma_{\rm stat}$ is the statistical error on A_1^ρ for the extended $p_{\rm t}^2$ sample. The uncertainty on the estimates of possible false asymmetries due to the time dependent effects is the dominant contribution to the total systematic error in most of the kinematical region.

Asymmetries for configurations where spin effects cancel out were calculated to check the cancellation of effects

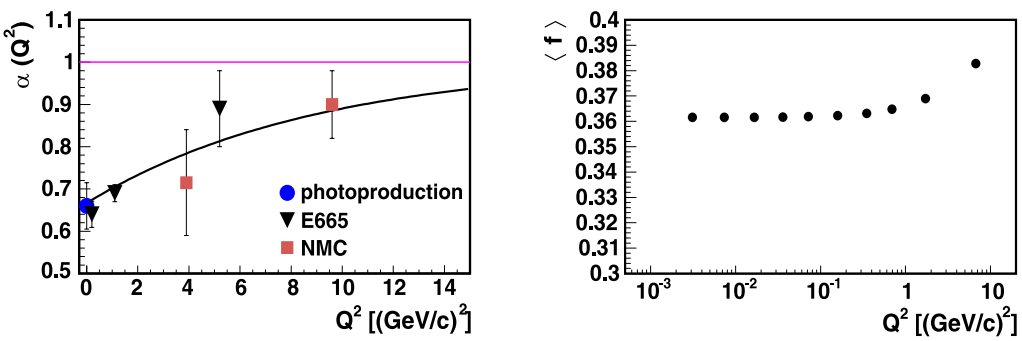

Fig. 4. (*Left*) Parameter α of (11) as a function of Q^2 (from [26]). The experimental points and the fitted curve are shown. See text for details. (*Right*) The dilution factor f as a function of Q^2

due to fluxes and acceptances. They were found to be compatible with zero within the statistical errors. Asymmetries obtained with different settings of the microwave (MW) frequency, used for DNP, were compared in order to test possible effects related to the orientation of the target magnetic field. The results for the extended p_t^2 sample tend to show that there is a small difference between asymmetries for the two MW configurations. However, because the numbers of events of the data samples taken with each MW setting are approximately balanced, the effect of this difference on A_1^ρ is negligible for the total sample.

The systematic error on A_1^ρ also contains an overall scale uncertainty of 6.5% due to uncertainties on P_B and P_T. The uncertainty of the parameterisation of $R(Q^2)$ affects the depolarisation factor D. The uncertainty of the dilution factor f is mostly due to uncertainty of the parameter $\alpha(Q^2)$, which takes into account nuclear effects in incoherent ρ^0 production. The neglect of the A_2^ρ term mainly affects the highest bins of Q^2 and x.

Another source of systematic errors is due to the contribution of the non-exclusive background to our sample. This background originates from two sources. The first one is due to the production of ρ^0 accompanied by the dissociation of the target nucleon, the second one is the production of ρ^0 in inclusive scattering. In order to evaluate the amount of background in the sample of exclusive events it is necessary to determine the E_{miss} dependence for the non-exclusive background in the region under the exclusive peak (cf. Fig. 1). For this purpose complete Monte Carlo simulations of the experiment were used, with events generated by either the PYTHIA 6.2 or LEPTO 6.5.1 generators. Events generated with LEPTO come only from deep inelastic scattering and cover the range of $Q^2 > 0.5\,(\mathrm{GeV}/c)^2$. Those generated with PYTHIA cover the whole kinematical range of the experiment and include exclusive production of vector mesons and processes with diffractive excitation of the target nucleon or the vector meson, in addition to inelastic production.

The generated MC events were reconstructed and selected for the analysis using the same procedure as for the data. In each bin of Q^2 the E_{miss} distribution for the MC was normalised to the corresponding one for the data in the range of large $E_{miss} > 7.5$ GeV. Then the normalised MC distribution was used to estimate the number of background events under the exclusive peak in the data. The fraction of background events in the sample of incoherent exclusive ρ^0 production was estimated to be about 0.12 ± 0.06 in most of the kinematical range, except in the largest Q^2 region, where it is about 0.24 ± 0.12. The large uncertainties of these fractions reflect the differences between estimates from LEPTO and PYTHIA in the region where they overlap. In the case of PYTHIA the uncertainties on the cross sections for diffractive photo- and electroproduction of vector mesons also contribute. For events generated

Table 1. Asymmetry A_1^ρ as a function of Q^2. Both the statistical errors (first) and the total systematic errors (second) are listed

Q^2 range	$\langle Q^2\rangle$ [$(\mathrm{GeV}/c)^2$]	$\langle x\rangle$	$\langle\nu\rangle$ [GeV]	A_1^ρ
0.0004–0.005	0.0031	4.0×10^{-5}	42.8	$-0.030\pm0.045\pm0.014$
0.005–0.010	0.0074	8.4×10^{-5}	49.9	$0.048\pm0.038\pm0.013$
0.010–0.025	0.017	1.8×10^{-4}	55.6	$0.063\pm0.026\pm0.014$
0.025–0.050	0.036	3.7×10^{-4}	59.9	$-0.035\pm0.027\pm0.009$
0.05–0.10	0.072	7.1×10^{-4}	62.0	$-0.010\pm0.028\pm0.008$
0.10–0.25	0.16	0.0016	62.3	$-0.019\pm0.029\pm0.009$
0.25–0.50	0.35	0.0036	60.3	$0.016\pm0.045\pm0.014$
0.5–1	0.69	0.0074	58.6	$0.141\pm0.069\pm0.030$
1–4	1.7	0.018	59.7	$0.000\pm0.098\pm0.035$
4–50	6.8	0.075	55.9	$-0.85\pm0.50\pm0.39$

Table 2. Asymmetry A_1^ρ as a function of x. Both the statistical errors (first) and the total systematic errors (second) are listed

x range	$\langle x\rangle$	$\langle Q^2\rangle$ [$(\mathrm{GeV}/c)^2$]	$\langle\nu\rangle$ [GeV]	A_1^ρ
8×10^{-6}–1×10^{-4}	5.8×10^{-5}	0.0058	51.7	$0.035\pm0.026\pm0.011$
1×10^{-4}–2.5×10^{-4}	1.7×10^{-4}	0.019	59.7	$0.036\pm0.024\pm0.010$
2.5×10^{-4}–5×10^{-4}	3.6×10^{-4}	0.041	61.3	$-0.039\pm0.027\pm0.012$
5×10^{-4}–0.001	7.1×10^{-4}	0.082	60.8	$-0.010\pm0.030\pm0.010$
0.001–0.002	0.0014	0.16	58.6	$-0.005\pm0.036\pm0.013$
0.002–0.004	0.0028	0.29	54.8	$0.032\pm0.050\pm0.019$
0.004–0.01	0.0062	0.59	50.7	$0.019\pm0.069\pm0.026$
0.01–0.025	0.015	1.3	47.5	$-0.03\pm0.14\pm0.06$
0.025–0.8	0.049	3.9	43.8	$-0.27\pm0.38\pm0.19$

with PYTHIA the E_{miss} distributions for various physics processes could be studied separately. It was found that events of ρ^0 production with an excitation of the target nucleon into N^* resonances of small mass, $M < 2\,\mathrm{GeV}/c^2$, cannot be resolved from the exclusive peak and therefore were not included in the estimates of the number of background events.

An estimate of the asymmetry A_1^ρ for the background was obtained using a non-exclusive sample, which was selected with the standard cuts used in this analysis, except the cut on E_{miss} which was modified to $E_{\mathrm{miss}} > 2.5$ GeV. In different high-E_{miss} bins, A_1^ρ for this sample was found to be compatible with zero.

Because no indication of a non-zero A_1^ρ for the background was found, and also, due to a large uncertainty of the estimated amount of background in the exclusive sample, no background corrections were made. Instead, the effect of background was treated as a source of systematic error. Its contribution to the total systematic error was not significant in most of the kinematical range, except for the highest Q^2 and x.

The total systematic error on A_1^ρ was obtained as a quadratic sum of the errors from all sources discussed. Its values for each Q^2 and x bin are given in Tables 1 and 2. The total systematic error amounts to about 40% of the statistical error for most of the kinematical range. Both errors become comparable in the highest bin of Q^2.

6 Results

The COMPASS results on A_1^ρ are shown as a function of Q^2 and x in Fig. 5 and listed in Tables 1 and 2. The statistical errors are represented by vertical bars and the total systematic errors by shaded bands.

The wide range in Q^2 covers four orders of magnitude from 3×10^{-3} to 7 $(\mathrm{GeV}/c)^2$. The domain in x that is strongly correlated with Q^2 varies from 5×10^{-5} to about 0.05 (see the tables for more details). For the whole kinematical range the A_1^ρ asymmetry measured by COMPASS is consistent with zero. As discussed in the introduction, this indicates that the role of unnatural-parity exchanges, like π– or A_1–Reggeon exchange, is small in that kinematical domain, which is to be expected if diffraction is the dominant process for reaction (2).

In Fig. 6 the COMPASS results are compared to the HERMES results on A_1^ρ obtained on a deuteron target [19]. Note that the lowest Q^2 and x HERMES points, referred to as 'quasi-photoproduction', come from measurements where the kinematics of the small-angle scattered electron was not measured but estimated from a MC simulation. This is in contrast to COMPASS, where scattered muon kinematics is measured even at the smallest Q^2.

The results from both experiments are consistent within errors. The kinematical range covered by the present analysis extends further towards small values of

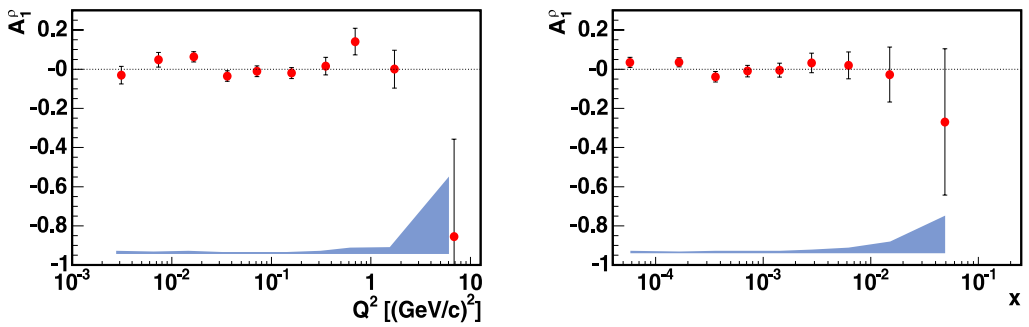

Fig. 5. A_1^ρ as a function of Q^2 (*left*) and x (*right*) from the present analysis. Error bars correspond to statistical errors, while the *bands* at the bottom represent the systematical errors

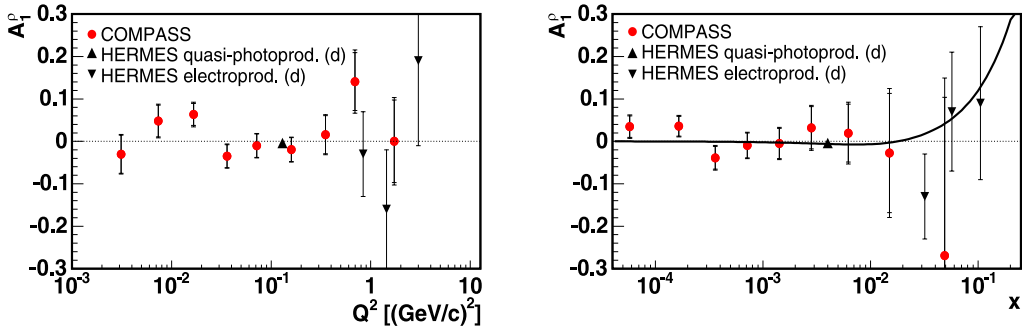

Fig. 6. A_1^ρ as a function of Q^2 (*left*) and x (*right*) from the present analysis (*circles*) compared to HERMES results on the deuteron target (*triangles*). For the COMPASS results *inner bars* represent statistical errors, while the *outer bars* correspond to the total error. For the HERMES results *vertical bars* represent the quadratic sum of statistical and systematic errors. The *curve* represents the prediction explained in the text

x and Q^2 by almost two orders of magnitude. In each of the two experiments A_1^ρ is measured at different average W, which is equal to about 10 GeV for COMPASS and 5 GeV for HERMES. Thus, no significant W dependence is observed for A_1^ρ on an isoscalar nucleon target.

The x dependence of the measured A_1^ρ is compared in Fig. 6 to the prediction given by (4), which relates A_1^ρ to the asymmetry A_1 for the inclusive inelastic lepton–nucleon scattering. To produce the curve the inclusive asymmetry A_1 was parameterised as $A_1(x) = (x^\alpha - \gamma^\alpha)(1 - \mathrm{e}^{-\beta x})$, where $\alpha = 1.158 \pm 0.024$, $\beta = 125.1 \pm 115.7$ and $\gamma = 0.0180 \pm 0.0038$. The values of the parameters have been obtained from a fit of $A_1(x)$ to the world data from polarised deuteron targets [28–33], including COMPASS measurements at very low Q^2 and x [34]. Within the present accuracy the results on A_1^ρ are consistent with this prediction.

In the highest Q^2 bin, $\langle Q^2 \rangle = 6.8\,(\mathrm{GeV}/c)^2$, in the kinematical domain of applicability of pQCD-inspired models that relate the asymmetry to the spin dependent GPDs for gluons and quarks (cf. the Introduction), one can observe a hint of a possible non-zero asymmetry, although with a large error. It should be noted that in [20] a negative value of A_{LL} different from zero by about two standard deviations was reported at $\langle Q^2 \rangle = 7.7\,(\mathrm{GeV}/c)^2$. At COMPASS, including the data taken with the longitudinally polarised deuteron target in 2004 and 2006 will result in an increase of statistics by a factor of about three compared to the present paper and thus may help to clarify the issue.

For the whole Q^2 range future COMPASS data, to be taken with the polarised proton target, would be very valuable for checking if the role of the flavour-blind exchanges is indeed dominant, as expected for the Pomeron-mediated process.

7 Summary

The longitudinal double spin asymmetry A_1^ρ for the diffractive muoproduction of the ρ^0 meson, $\mu + N \to \mu + N + \rho$, has been measured by scattering longitudinally polarised muons off longitudinally polarised deuterons from the ^{6}LiD target and selecting incoherent exclusive ρ^0 production. The presented results for the COMPASS 2002 and 2003 data cover a range of energy W from about 7 to 15 GeV.

The Q^2 and x dependence of A_1^ρ is presented in a wide kinematical range, $3 \times 10^{-3} \leq Q^2 \leq 7\,(\mathrm{GeV}/c)^2$ and $5 \times 10^{-5} \leq x \leq 0.05$. These results extend the range in Q^2 and x by two orders of magnitude down with respect to the existing data from HERMES.

The asymmetry A_1^ρ is compatible with zero in the whole x and Q^2 range. This may indicate that the role of unnatural-parity exchanges like π– or A_1–Reggeon exchange is small in that kinematical domain.

The x dependence of the measured A_1^ρ is consistent with the prediction of [13], which relates A_1^ρ to the asymmetry A_1 for inclusive inelastic lepton–nucleon scattering.

Acknowledgements. We gratefully acknowledge the support of the CERN management and staff and the skill and effort of the technicians of our collaborating institutes. Special thanks are due to V. Anosov and V. Pesaro for their support during the installation and the running of the experiment. This work was made possible by the financial support of our funding agencies.

References

1. K. Schilling, G. Wolf, Nucl. Phys. B **61**, 381 (1973)
2. NMC Collaboration, M. Arneodo et al., Nucl. Phys. B **429**, 503 (1994)
3. E665 Collaboration, M.R. Adams et al., Z. Phys. C **74**, 237 (1997)
4. ZEUS Collaboration, J. Breitweg et al., Eur. Phys. J. C **12**, 393 (2000)
5. H1 Collaboration, C. Adloff et al., Eur. Phys. J. C **13**, 371 (2000)
6. H1 Collaboration, C. Adloff et al., Phys. Lett. B **539**, 25 (2002)
7. HERMES Collaboration, K. Ackerstaff et al., Eur. Phys. J. C **18**, 303 (2000)
8. A. Sandacz (on behalf of the COMPASS Collaboration), Nucl. Phys. B Proc. Suppl. **146**, 581 (2005)
9. I.P. Ivanov, N.N. Nikolaev, JETP Lett. C **29**, 294 (1999)
10. I.P. Ivanov, Diffractive production of vector mesons in Deep Inelastic Scattering within k_t-factorization approach, hep-ph/0303053
11. S.I. Manaenkov, Regge description of spin–spin asymmetry in photon diffractive dissociation, Preprint DESY 99-016 [hep-ph/9903405]
12. H. Fraas, Nucl. Phys. B **113**, 532 (1976)
13. HERMES Collaboration, A. Airapetian et al., Phys. Lett. B **513**, 301 (2001)
14. J.C. Collins, L. Frankfurt, M. Strikman, Phys. Rev. D **56**, 2982 (1997)
15. A.D. Martin, M.G. Ryskin, T. Teubner, Phys. Rev. D **55**, 4329 (1997)
16. M.G. Ryskin, Phys. Atom. Nucl. **62**, 315 (1999) [Yad. Fiz. **62**, 350 (1999)]
17. S.V. Goloskokov, P. Kroll, Eur. Phys. J. C **42**, 281 (2005)
18. S.V. Goloskokov, P. Kroll, hep-ph/0611290
19. HERMES Collaboration, A. Airapetian et al., Eur. Phys. J. C **29**, 171 (2003)
20. A. Tripet, Nucl. Phys. B Proc. Suppl. **79**, 529 (1999)
21. COMPASS Collaboration, P. Abbon et al., Nucl. Instrum. Methods A **577**, 455 (2007)
22. J. Kiryluk, Ph.D. thesis, Warsaw University, 2000
23. SMC Collaboration, D. Adams et al., Phys. Rev. **56**, 5330 (1997)
24. E665 Collaboration, M.R. Adams et al., Phys. Rev. Lett. **74**, 1525 (1995)
25. T. Bauer et al., Rev. Mod. Phys. **50**, 261 (1978) [Erratum ibid **51**, 407 (1979)]
26. A. Tripet, Ph.D. thesis, Universität Bielefeld, 2002
27. K. Kurek, QED radiative corrections in exclusive ρ^0 leptoproduction, preprint DESY-96-209, June 1996 [hep-ph/9606240]
28. SMC Collaboration, B. Adeva et al., Phys. Rev. D **58**, 112 001 (1998)

29. E143 Collaboration, K. Abe et al., Phys. Rev. D **58**, 112 003 (1998)
30. E155 Collaboration, P.L. Anthony et al., Phys. Lett. B **463**, 339 (1999)
31. SMC Collaboration, B. Adeva et al., Phys. Rev. D **60**, 072 004 (1999) [Erratum ibid **62**, 079 902 (2000)]
32. HERMES Collaboration, A. Airapetian et al., Phys. Rev. D **75**, 012 007 (2007)
33. COMPASS Collaboration, V.Y. Alexakhin et al., Phys. Lett. B **647**, 8 (2007)
34. COMPASS Collaboration, V.Y. Alexakhin et al., Phys. Lett. B **647**, 330 (2007)